

α clustering in ^{208}Pb from $(d, {}^6\text{Li})$ at $E_d = 55$ MeV

F. D. Becchetti, J. Jänecke, and D. Overway

Department of Physics, University of Michigan, Ann Arbor, Michigan 48109

J. D. Cossairt*

Cyclotron Institute, Texas A & M University, College Station, Texas 77843

R. L. Spross

Department of Physics, University of Southwestern Louisiana, Lafayette, Louisiana 70504

(Received 27 November 1978)

The reaction $^{208}\text{Pb}(d, {}^6\text{Li})^{204}\text{Hg}$ has been observed at $E_d = 55$ MeV. Data for several levels in ^{204}Hg up to $E_x \simeq 3.5$ MeV have been obtained and alpha-particle spectroscopic factors and reduced alpha widths for ^{208}Pb deduced with distorted-wave Born approximation analyses. The reduced alpha widths have been utilized to deduce the "alpha decay" properties of ^{208}Pb , as well as superheavy nuclei. The analysis indicates $\log T_{1/2}^\alpha$ (years) = 127.4 ± 1.0 for ^{208}Pb and $\log T_{1/2}^\alpha$ (years) = 2.5 ± 2.0 for $Z = 114$, $N = 184$ and $Q_\alpha = 7.0 \pm 0.5$ MeV. The results also imply that about 1% of the protons in ^{208}Pb at $r = 10$ fm are associated with alpha clusters.

NUCLEAR REACTIONS $^{208}\text{Pb}(d, {}^6\text{Li})^{204}\text{Hg}$, $E = 54.8$ MeV; measured $\sigma(\theta)$. ^{204}Hg deduced levels, S_α , $\gamma_\alpha^2(10 \text{ fm})$. DWBA analyses. Magnetic spectrometer.

I. INTRODUCTION

It has been suggested that α clustering is an important feature of low density regions of nuclei ($\rho/\rho_0 \lesssim 1\%$). Thus far most experimental data on α clustering have come from a study of α decay,^{1,2} pre-equilibrium α emission,³ α -knockout reactions,⁴ and direct α -transfer reactions.⁵ Except for α -decay studies, most reaction data have been limited to light nuclei. It has recently been demonstrated⁶⁻⁹ that studies of direct α -transfer reactions such as $(d, {}^6\text{Li})$ and $({}^{16}\text{O}, {}^{12}\text{C})$ are feasible for nuclei $A > 100$. The $(d, {}^6\text{Li})$ reaction, in particular, has several advantageous features: Firstly, $J^\pi(g.s.) \rightarrow 0^+$ transitions are easily observable and possess distinctive diffractive angular distributions; secondly, most nuclei beyond $A > 150$ have positive α -decay energies i.e., $Q_\alpha > 0$, so the $(d, {}^6\text{Li})$ Q values are favorable in even the heaviest nuclei. The fact that $Q > 0$ implies that most heavy nuclei are in principle "unstable" to α decay. A study of $(d, {}^6\text{Li})$ then permits one to extract the α -decay properties of these nuclei.⁷

Finally, extraction of α -spectroscopic factors S_α and reduced α widths γ_α^2 , is of interest in view of the recent development of various techniques based on group theory,^{10,11} the interacting boson model,^{12,13} and the pairing vibrational model,¹⁴ which simplify calculation of S_α from nuclear wave functions. While most of these techniques are applicable to heavy nuclei, they have thus far been applied mainly to light nuclei ($A < 100$).

In this paper we report on $^{208}\text{Pb}(d, {}^6\text{Li})^{204}\text{Hg}$ at

$E_d = 55$ MeV. Data obtained for ^{238}U and ^{232}Th targets in the same experiment will be reported elsewhere.

II. EXPERIMENTAL PROCEDURES

An energy analyzed 54.8 MeV deuteron beam produced at the Texas A&M cyclotron was utilized together with an Enge split-pole magnetic spectrometer ($\Delta\Omega = 2.1$ msr, $\Delta\theta = 3^\circ$). The reaction products were identified in the focal plane of the spectrometer with a gas proportional counter backed by a 5 cm wide \times 1 cm high silicon solid-state detector. The gas counter provided energy loss (ΔE) and position (x) signals. The solid-state detector provided an energy (E) signal. It was biased just to stop the ions of interest (${}^6\text{Li}^{3+}$) and thus reduce the energy signals from the more abundant lighter reaction products such as α particles. The time of flight of reaction products through the spectrometer was obtained from signals derived from the solid-state detector and the cyclotron rf pulse. The detector proved capable of good particle discrimination in the presence of an intense background of other ions mostly deuterons and α particles. The detector system was calibrated in energy using deuteron elastic scattering or ${}^{12}\text{C}(d, {}^6\text{Li})^8\text{Be}$. The effective detector width along the focal plane corresponded to 1.6 MeV excitation energy in ^{204}Hg . The limited vertical aperture of the solid-state detector resulted in an overall efficiency of 60% to 95%, depending on the beam spot size. Although this

efficiency was determined before each set of runs, some uncertainty in the quoted cross reactions ($\pm 10\%$) is introduced. Computer dead time was monitored and kept below 10%.

Typical beam intensity was $>1.5 \mu\text{A}$, which necessitated use of a water-cooled carbon beam stop which was located inside the scattering chamber. Owing to the water cooling, the Faraday cup was not completely isolated electrically and it was necessary to compensate for a small leakage current. The compensated current was then checked against readings on other beam stops and generally agreed to within $\pm 10\%$.

The targets consisted of self-supporting foils of enriched ^{208}Pb ($>99\%$). The thickness and uniformity of the targets was determined by α -particle energy loss ($E_\alpha = 5.5 \text{ MeV}$) and the average thicknesses measured by determining the weight to area ratio before and after a run. The various methods gave results which agreed to about 25% for two different targets ($\rho x = 1.6$ and 2.0 mg/cm^2). The energy resolution in this experiment was limited by the thick targets employed to 150 to 300 keV, full width at half maximum (FWHM).

The combined uncertainties in the Faraday-cup current, detector acceptance, and target thicknesses yield an estimated uncertainty of $\pm 30\%$ in the absolute cross sections.

III. DATA

Spectra obtained for $^{208}\text{Pb}(d, ^6\text{Li})^{204}\text{Hg}$ are displayed in Fig. 1. The spectrum observed for $^{208}\text{Pb}(d, ^6\text{Li})$ is very similar to spectra obtained for other doubly closed-shell nuclei: ^{16}O , ^{40}Ca , ^{90}Zr namely, increasing α -transfer strength with increasing spin and excitation energy.⁵ This is distinctly different from the situation observed for $(d, ^6\text{Li})$ on other nuclei.^{7,15} Only the 0^+ g.s. and 2^+ levels in ^{204}Hg have been assigned spins based on previous measurements. The cross sections observed for $^{208}\text{Pb}(d, ^6\text{Li})$ at $E_d = 55 \text{ MeV}$ ($d\sigma/d\Omega_{\text{g.s.}} \sim 0.4 \mu\text{b/sr}$) are substantially larger than those measured for ^{208}Pb at $E_d = 35 \text{ MeV}$ (Ref. 6) ($d\sigma/d\Omega_{\text{g.s.}} \approx 50 \text{ nb/sr}$) and those observed^{6,16} for ^{238}U and ^{232}Th at $E_d = 35$ and 55 MeV ($d\sigma/d\Omega_{\text{g.s.}} < 100 \text{ nb/sr}$). In fact, the cross sections for ^{208}Pb at $E_d = 55 \text{ MeV}$ are not much less than observed for some sd -shell nuclei.^{5,6}

The excitation energies for levels observed in ^{204}Hg in the present experiment are listed in Table I. They are believed to be accurate to $\pm 50 \text{ keV}$. As noted in the Introduction, the Q value for $(d, ^6\text{Li})$ in heavy nuclei is positive, which excludes ^6Li groups arising from light contaminants. Thus ^6Li groups observed at $E_x = 2.24, 2.74, 2.8, 3.0,$ and 3.6 MeV are presumed to originate from lev-

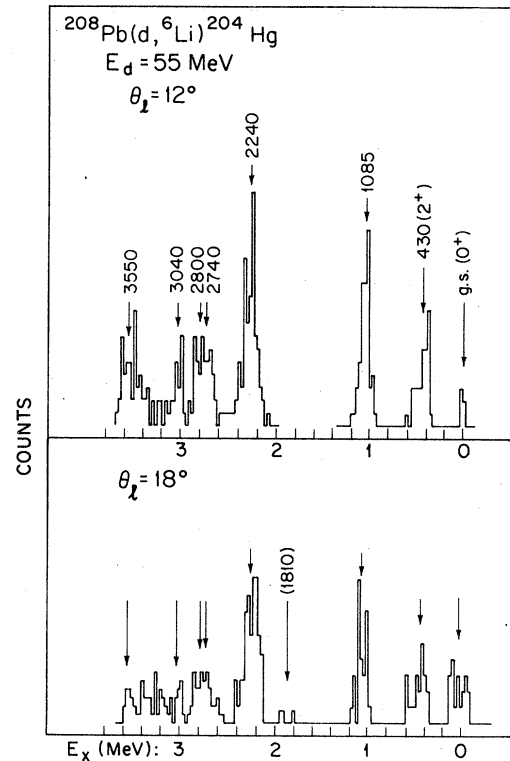


FIG. 1. Spectra at $l=0$ minimum (top) and maximum (bottom).

els in ^{204}Hg , although in some cases the groups observed may be from more than one level.

Angular distributions obtained for states in ^{204}Hg at $E_x = 0.00, 0.43,$ and 1.085 MeV are displayed in Figs. 2 and 3. The calculated curves are discussed in Sec. IV. Data at three angles were also obtained for the groups at $E_x > 1.6 \text{ MeV}$ to facilitate their identification (see Table I).

The data obtained for the lowest three levels appear consistent with $J^\pi = 0^+, 2^+, \text{ and } 4^+$, respectively. The group observed at $E_x = 1.81 \text{ MeV}$ is of uncertain origin as it was observed at only two angles which correspond to $l=0$ maxima. The data would thus be consistent with a $J^\pi = 0^+$ level but we cannot exclude the possibility that this group arises from the trace amounts ($< 1\%$) of ^{207}Pb and ^{206}Pb in the target as the Q values and kinematic shifts are similar for these nuclei. The transition, if due to one of these nuclei, would be $\times 20$ more intense than any observed in $^{208}\text{Pb}(d, ^6\text{Li})$, however.

The limited data for the strong transition to the level at $E_x = 2.24 \text{ MeV}$ suggest $J \geq 3$, while data for the other levels suggest $J \geq 2$. These J values are based on the observed ratio of cross sections at various angles relative to data for the presumed $0^+, 2^+, \text{ and } 4^+$ levels, together with, distorted-

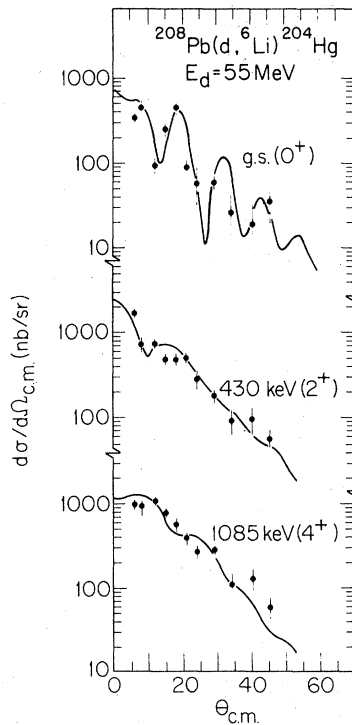


FIG. 2. Measured angular distributions and associated random errors. The estimated absolute error is $\pm 30\%$ (see text). The curves are finite-range DWBA calculations employing our adopted parameter set (FRDW-2, Table II).

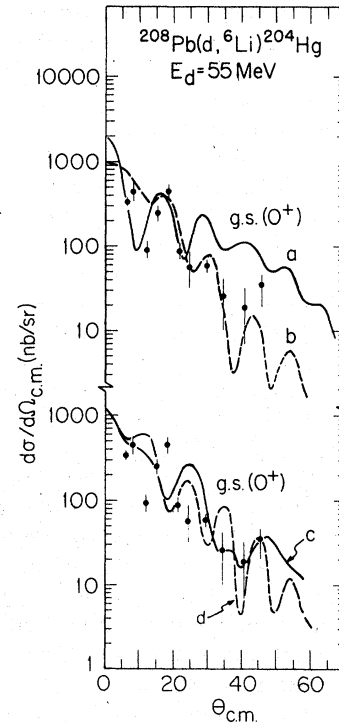


FIG. 3. Measured g.s. angular distribution compared with DWBA calculations as in Fig. 1 except as follows: (a) $\alpha+d$ and $\alpha+^{204}\text{Hg}$ potentials similar to those of Ref. 25 ($N, L=0, 0$) and Ref. 34 ($N, L=9, 0$) respectively; (b) $\alpha+d$ wave function, Ref. 25, with a "folded" type $^{204}\text{Hg}+\alpha$ potential ($r_0=1.10$ fm and $a=0.82$ fm); (c) $\alpha+d$ wave function from Ref. 24 ($N, L=1, 0$) with $^{204}\text{Hg}+\alpha$ potential as employed in Ref. 7 ($r_0=1.30$ fm, $a=0.73$ fm); (d) same as (c) except $V_{so}=0$ in the deuteron optical potential.

TABLE I. Experimental data, $^{208}\text{Pb}(d, ^6\text{Li})^{204}\text{Hg}$ $E_d = 54.8$ MeV.

E_x^a	J^π^b	$d\sigma/d\Omega(\theta_l=18^\circ)^c$	R^c	σ^d
		($\mu\text{b}/\text{sr}$)		(μb)
g.s.	0^+	0.45 ± 0.10	0.20 ± 0.03	0.17
430	2^+	0.74 ± 0.04	1.54 ± 0.26	0.50
1085	(4^+)	1.07 ± 0.06	1.90 ± 0.36	0.54
(1810) ^e		$(0.06 \pm 0.04)^e$	$<0.2)^e$	
2240	f	1.60 ± 0.07	1.06 ± 0.11	(1.1) ^g
2740	f	0.62 ± 0.09	1.62 ± 0.22	(0.5) ^g
+2800				
3040	f	0.82 ± 0.11	0.78 ± 0.17	(0.5) ^g
3550	f	0.55 ± 0.07	0.54 ± 0.10	(0.3) ^g

^aPresent experiment, ± 50 keV.

^bThis experiment and Ref. 17.

^cDifferential cross section at $l=0$ maximum (18° lab) and the ratio, $R \equiv d\sigma/d\Omega_{\text{c.m.}}(\theta_l=12^\circ)/d\sigma/d\Omega_{\text{c.m.}}(\theta_l=18^\circ)$ where $\theta_l=12^\circ$ is an $l=0$ minimum (see Fig. 1).

^dIntegrated cross section $\theta_{\text{c.m.}}=0^\circ$ to 50° . Uncertainty $\pm 30\%$.

^eOrigin of this group is uncertain as it is only seen at two angles (see text).

^fBased on the ratio R , these levels are likely not $J^\pi=0^+$.

^gEstimate based on limited data.

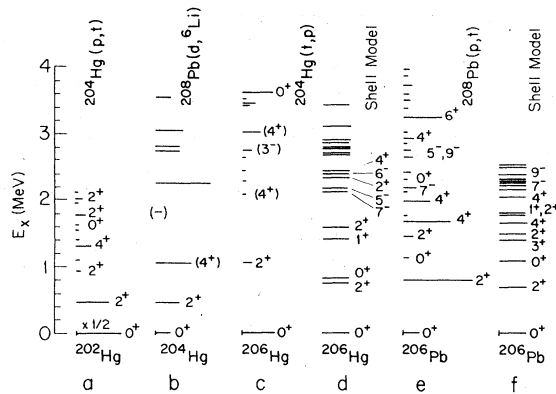


FIG. 4. Comparison of (p,t) , (t,p) , and $(d,{}^6\text{Li})$ with shell model calculations for nuclei $A=204\pm 2$. The maximum cross sections for the transfer reactions are indicated by the length of the lines shown. Uncertain assignments are indicated by parentheses: (a) Ref. 17; (b) this work; (c) Ref. 18; (d) Ref. 20; (e) Ref. 19; (f) Ref. 20.

wave Born-approximation (DWBA) calculations for other J^π values (see Sec. V).

The excitation energies of levels in ${}^{204}\text{Hg}$ are compared with those for nearby Hg and Pb isotopes¹⁷⁻¹⁹ in Fig. 4. Although one may make a correspondence with many of the levels in Hg and Pb, one should first note the following features⁷⁻¹⁵ of levels populated with $(d,{}^6\text{Li})$: Unnatural parity states (1^+ , 3^+ , 2^- , ...) cannot be populated directly in a single step; 0_2^+ and 2_2^+ two quasiparticle levels tend to be weak while the corresponding 4_1^+ member may be strong; certain negative parity levels (3^- – 9^-) may be favored, particularly the “stretched” configurations, $(\nu^{-2})_{0^+} \otimes (\pi^{-2})_{J_{\max}}$, or vice versa, where $J_{\max} = (I_1 \pm \frac{1}{2}) + (I_2 \mp \frac{1}{2})$.

In general, one can often correlate levels observed in $(d,{}^6\text{Li})$ with those observed in two-nucleon transfer leading to the same nuclei. We thus compare (p,t) and (t,p) in neighboring nuclei with $(d,{}^6\text{Li})$ in Fig. 4. ${}^{208}\text{Pb}(p,t){}^{206}\text{Pb}$ at $E_p = 40$ MeV populates primarily the $0_1^+(\text{g.s.})$, 2_1^+ (0.8 MeV), 4_1^+ (1.68 MeV), 4_2^+ (1.99 MeV), and 7^- (2.2 MeV) levels and several other high-spin levels, $E_x > 2.5$ MeV.¹⁹ This is consistent with $J^\pi = 4_1^+$ for the 1.085 MeV ${}^{204}\text{Hg}$ level excited in $(d,{}^6\text{Li})$. Also, a weak 0_3^+ ($E_x = 2.3$ MeV) neutron-pairing vibration observed in (p,t) could correspond to the possible “ 0^+ ” level seen in ${}^{204}\text{Hg}$ at $E_x = 1.81$ MeV. Similarly, ${}^{204}\text{Hg}(p,t){}^{202}\text{Hg}$ at $E \approx 18$ MeV populates the $0^+(\text{g.s.})$, 2_1^+ (440 keV), 4^+ (1.31 MeV), 0^+ (1.64 MeV), and several 2^+ levels, $E_x > 1.6$ MeV. Negative parity levels (5^- , 7^- , 9^-) apparently are not observed, possibly due to the low bombarding energy which favors low l transfers. The low-lying 2_1^+ and 4_1^+ levels predicted and observed with (p,t) in ${}^{206}\text{Hg}$ (Fig. 4) tend to be at higher exci-

tation due to the closed neutron shell, while the negative parity levels are affected much less.

Shell model calculations²⁰ as well as data for the γ decay of various Hg and Pb isotopes²¹ indicate the likely presence of low-lying negative parity states in ${}^{204}\text{Hg}$ and other Hg and Pb isotopes. The calculations of Ma and True²⁰ for ${}^{206}\text{Hg}$ predict 5^- and 7^- levels at $E_x \approx 2.4$ MeV. Among these levels are several “stretched” configurations such as $(\pi d_{3/2}^{-1} \pi h_{11/2}^{-1})_{7^-} \otimes (\nu^{-2})_{0^+}$, $(\nu p_{1/2}^{-1})_{7^-} \otimes (\pi^{-2})_{0^+}$, and $(\nu f_{5/2}^{-1} \nu i_{13/2}^{-1})_{9^-} \otimes (\pi^{-2})_{0^+}$. The analogous $(\nu d_{3/2}^{-1} \nu h_{11/2}^{-1})_{7^-} \otimes (\pi^{-2})_{0^+}$ configuration is observed in $\text{Te}(d,{}^6\text{Li})$ with the companion $J^\pi = 5^-$ level somewhat weaker.¹⁵ It appears probable that the level (or levels) at $E_x = 2.24$ in ${}^{204}\text{Hg}$ is one or more of these configurations, probably $J^\pi = 7^-$ and/or 9^- , of the form ${}^{206}\text{Hg}(0^+\text{g.s.}) \otimes {}^{206}\text{Pb}(E_x)$ or ${}^{206}\text{Pb}(0^+\text{g.s.}) \otimes {}^{206}\text{Hg}(E_x)$. We may also attribute the strength observed for other groups as due to less-favored members of the negative parity levels (3^- , 5^-) which should be at higher excitation. It has been observed^{7,15} that within multiplets the levels lowest in excitation energy also collect most of the α -transfer strength. This is not unexpected, owing to the short range nature of nuclear interactions which affects binding energy and α clustering in a similar fashion.

The above discussion is intended as a guide for future studies of ${}^{204}\text{Hg}$. It should not be interpreted as assigning spins of levels observed in ${}^{204}\text{Hg}$.

IV. ANALYSIS

A. α spectroscopic factors

The angular distributions have been analyzed with finite-range Born approximation²²⁻²⁴. Various sets of deuteron and ${}^6\text{Li}$ optical potentials were investigated²⁵⁻²⁹ and except for the absolute S_α values, these gave generally similar angular distributions at forward angles. Spin-orbit coupling in the deuteron channel, unlike that in ${}^6\text{Li}$ channel, had a significant effect (Fig. 3) and was therefore included. Our adopted optical parameters are listed in Table I.

The α -transfer form factor was generated with α -cluster wave functions produced in a Wood-Saxon potential well. The α -cluster quantum numbers for ${}^{204}\text{Hg} + \alpha$ were taken as $2N + L = 18$ with the α -binding energy set to the α -separation energy or, for unbound levels, 0.5 MeV. Some calculations also employed resonant wave functions.⁷ The $\alpha + d$ wave function for ${}^6\text{Li}$ was initially generated using the potential suggested by Kubo and Hirata²⁴ ($N, L = 1, 0$). The calculations with this wave function, however, appeared to be consistently out of phase with the data [Fig. 3(c)]. We

TABLE II. α spectroscopic factors, widths and half-life, $^{208}\text{Pb} \rightarrow \alpha + {}^{204}\text{Hg}$.

E_x (MeV) $E_d = 55$ MeV	J^π ^a	N, L ^a	Abs. FRDW-1 ^b		Abs. FRDW-2 ^c		Norm. ZRDW-1 ^d		Norm. FRDW-2 ^e		$\log T_{1/2}^\alpha$ ^f (yr)
			S_α	γ_α^2 (keV)	S_α	γ_α^2 (keV)	S_α	γ_α^2 (keV)	S_α	γ_α^2 (keV)	
g.s.	0^+	9, 0	0.30	0.24	6.0	0.27	0.014	0.007	1.0	0.043	127.4 ± 1.0
0.430	2^+	8, 2	0.83	0.46	15.1	0.53	0.04	0.02	2.5	0.085	
1.085	4^+	7, 4	0.78	0.34	17.6	0.36	0.04	0.02	2.8	0.058	
(1.81)	(0^+)	(9, 0)	0.05	0.02	0.9	0.04	0.003	0.001	0.2	0.006	
2.240	(7^-)	(6, 7)	5.2	0.63	27.6	0.29	0.14	0.03	4.5	0.047	
2.74	(5^-)	(7, 5)	0.7	0.13	9	0.16	0.05	0.02	1.5	0.03	
+2.80											
3.04	(5^-)	(7, 5)	0.7	0.13	8	0.15	0.05	0.02	1.3	0.02	
3.55	(5^-)	(7, 5)	0.3	0.06	6	0.10	0.03	0.01	1.0	0.01	
$E_d = 35$ MeV											
g.s.	0^+	9, 0	0.10	0.08	1.0	0.04	0.002	0.002	0.2	0.007	128.2 ± 1.0

^a Assumed spin, parity, and α -cluster quantum numbers of the indicated levels in ^{204}Hg . The J^π values given in parentheses are for calculational purposes only as the data do not permit spin assignment other than certain limits (see text). The calculations for integrated cross sections are relatively insensitive to the J value, however (less than $\times 2$).

^b Absolute α spectroscopic factor and reduced α width (channel radius = 10 fm), determined by fits to angle-integrated cross sections (Table I). The ${}^6\text{Li}$ optical potentials are from Ref. 28: $V_R = 240$ MeV, $R_R = 7.65$ fm, $a_R = 0.65$ fm, $W_V = 12.0$ MeV, $R_I = 10.0$ fm, $a_I = 0.90$ fm, $V_{SO} = 0$. The deuteron optical potentials are from Ref. 27, set E: $V_R = 90.7$ MeV, $R_R = 6.81$ fm, $a_R = 0.79$ fm, $W_V = 2.4$ MeV, $W_D = 11.3$ MeV, $R_I = 7.88$ fm, $a_I = 0.89$ fm, $V_{SO} = 5.5$ MeV, $R_{SO} = 6.52$ fm, $a_{SO} = 0.55$ fm. The calculations denoted FRDW-1 are absolute finite-range DWBA (Ref. 22) utilizing the $\alpha + d$ wave function of Kubo and Hirata (Ref. 24; $N, L = 1, 0$; ${}^6\text{Li}$ $S_\alpha = 1.0$) and an $\alpha + {}^{204}\text{Hg}$ potential with $r_0 = 1.30$ fm, $a = 0.73$ fm (Ref. 7). The calculations FRDW-1 do not yield good fits to the angular distributions (Fig. 3). The values listed for the "1.81", 2.74 + 2.80, 3.04, and 3.55 MeV levels are estimates based on interpolations of other calculations.

^c Same as b except an α - d wave function similar to that specified by Watson has been used (Ref. 25; $N, L = 0, 0$; $S_\alpha = 1.0$) together with an $\alpha + {}^{204}\text{Hg}$ potential $r_0 = 1.20$ fm, $a = 0.65$ fm. This parameter set yields the best fit to the angular distributions (Fig. 2).

^d Zero-range DWBA normalized to $^{148}\text{Sm}(d, {}^6\text{Li})$ such that $\gamma_\alpha^2(9\text{ fm}) = 0.79$ keV for ^{148}Sm g.s. as deduced from the α decay of ^{148}Sm with $r_0 = 1.3$ fm, $a = 0.73$ fm (Refs. 7, 15). The normalization employed is $N = 6.7$ (Ref. 15).

^e Same as c except the calculations have been renormalized to $^{148}\text{Sm}(d, {}^6\text{Li})$ and $\gamma_\alpha^2(9\text{ fm}) = 1.07$ keV for ^{148}Sm g.s. obtained with $r_0 = 1.2$ fm, $a = 0.65$ fm.

^f Half-life for α decay. The value listed corresponds to the α width and penetrability inferred from the calculation Norm. FRDW-2 described in e, while the errors span the results obtained using the other parameter sets. (The value $\log T_{1/2}^\alpha = 129.7$ given in Ref. 7 contains a numerical error and should be $\log T_{1/2}^\alpha = 128.3$ for $r_0 = 1.30$ fm, $a = 0.73$ fm).

subsequently adopted an $\alpha + d$ wave function similar to that used by Watson *et al.*²⁵ in analysis of α knockout from ${}^6\text{Li}$. This wave function was generated with $N, L = 0, 0$ with a potential having a "soft" inner core ($V_{\alpha d}$ and $\Phi_{\alpha d} \approx 0$, $r_{\alpha d} < 1$ fm) to simulate proper antisymmetrization. It is thus thought to be a more realistic representation of an $\alpha + d$ cluster wave function with $N, L = 1, 0$ but with a suppressed inner node and has been shown to reproduce a wide range of data.²⁵

The choice of the $\alpha + {}^{204}\text{Hg}$ potential also proved not to be arbitrary (Fig. 3). Instead, certain geometries were found to improve simultaneously the DWBA fits for data with $l = 0, 2$, and 4, in particular $r_0 \approx 1.20$ fm.

Similar effects to those noted above have been observed in analyses of $({}^6\text{Li}, d)$, $A < 90$,²⁶ and $(d, {}^6\text{Li})$, $A \approx 120$.¹⁵

Curves obtained with our adopted parameter sets are shown in Fig. 2 and the results are listed in Table II. The $\alpha + {}^{204}\text{Hg}$ potential ($r_0 = 1.20$ fm, $a = 0.65$ fm) resembles nucleon-nucleus³⁰ and α -nucleus potentials^{31,32} derived from fitting high ener-

gy scattering data rather than potentials determined from low energy α scattering ($r_0 \approx 1.30$ fm, $a \approx 0.65$ fm).^{33,34} It also resembles folded α -nucleus potentials.³²

The α -spectroscopic factors deduced for $^{208}\text{Pb} \rightarrow \alpha + {}^{204}\text{Hg}$ are given in Table II. These have been calculated with two different methods: the first, based entirely on absolute finite-range DWBA calculations, indicates $S_\alpha(\text{g.s.}) \approx 6.0$ for $r_0 = 1.20$ fm, $a = 0.65$ fm (abs. FRDW-2, Table II). The second method, using data from $^{148}\text{Sm}(d, {}^6\text{Li})$ and ^{148}Sm α decay as a normalization^{7,15}, effectively removes most of the dependence of S_α associated with the $\alpha + d$ wavefunction and to some extent the optical model parameters. This second method yields $S_\alpha(\text{g.s.}) \approx 1.0$ for our adopted parameter set (Norm. FRDW-2, Table II). Both values deduced here, which correspond to $r_0 = 1.20$ fm and $a = 0.65$ fm, are larger ($\times 6$) than those deduced using the limited data at 35 MeV with the same bound state parameters.

S_α values deduced for $^{208}\text{Pb} \rightarrow \alpha + {}^{204}\text{Hg}$ are 10^4 times larger than those from simple shell model

calculations.¹ One must include coherently many shell model configurations (>200) in order to reproduce such large S_α values.¹⁵

B. Reduced widths and half-life

The problems associated with the model dependence of S_α can be avoided to a large extent by use of reduced α widths as these are the quantities better determined in the ($d, {}^6\text{Li}$) reaction analysis.⁷ Also, one can then combine these with a calculated α penetrability to infer the α -decay properties of the target nucleus, in this case a stable nucleus, ${}^{208}\text{Pb}$.

The techniques employed here for extracting reduced widths and the choice of channel radius are described elsewhere^{7,15}. The reduced widths, $\gamma_\alpha^2(s=10\text{ fm})$, are given in Table II. Again, these have been obtained using two methods: absolute FRDW and normalization to the experimental α -decay width of ${}^{148}\text{Sm}$. In the latter instance we employ the same type of α -cluster bound state parameters for ${}^{148}\text{Sm}$ and ${}^{208}\text{Pb}$ and hence the relative α widths should be fairly accurate.

One observes that although S_α varies by a factor of 100 for various combinations of target and projectile α -cluster wave functions, the reduced α widths extracted with a given method agree to within a factor of 2. Again, however, there is a factor of $\times 10$ to $\times 30$ difference between widths extracted from FRDW and those deduced from normalization to the ${}^{148}\text{Sm}$ α -decay width (Table II). The latter are perhaps less model dependent; they depend little on the ${}^6\text{Li}$ wave function employed. The calculation of the α -penetrability, however, depends on the shape of the α -cluster potentials assumed.^{2,7,15}

The half-life extracted for ${}^{208}\text{Pb} \rightarrow \alpha + {}^{204}\text{Hg}$ from the inferred reduced α width and calculated penetrability is shown in Table II. Also listed are values deduced from limited data at $E_d = 35$ MeV. The long half-life deduced for ${}^{208}\text{Pb}$ is mostly due to the small penetrability as $Q_\alpha = 0.52$ MeV, although the reduced α width is also required and directly affects the decay rate.^{2,7}

C. α -clustering in ${}^{208}\text{Pb}$

The α -reduced widths (Table II) are directly related to the α particle density $\rho_\alpha^{N,L}(s)$ at a particular channel radius, s . We use N, L to denote that the α particle is in a particular quantum state, analogous to single-nucleon densities. Similarly, the total α -particle density will be an appropriate

sum of $\rho_\alpha^{N,L}(s)$. We may assume, however, that a lower limit for $\rho_\alpha(s) = \sum_{N,L} \rho_\alpha^{N,L}(s)$ may be obtained for large values of s by summing over the valence α clusters, i. e., the largest N and L values. Taking $\rho_\alpha^{N,L}(s) = S_\alpha^{N,L} |R_\alpha^{N,L}(s)|^2 / 4\pi$, where $\sqrt{S_\alpha} R_\alpha^{N,L}(s)$ is the $\alpha + {}^{204}\text{Hg}$ cluster wave function deduced from the reaction analysis of the experimental data at $E_d = 55$ MeV, implies $\rho_\alpha(10\text{ fm}) = 10^{-6 \pm 0.5}$ α particles/fm³. The limits indicated correspond to the range in the reduced α widths extracted with different techniques (Table II). As noted previously, the reduced α width is proportional to $S_\alpha |R_\alpha(s)|^2$ and hence $\gamma_\alpha^2(s)$ and $\rho_\alpha(s)$ are relatively model independent to within the limits indicated, i. e., $\times 10$.

The above result for $\rho_\alpha(s)$ is to be compared with the total proton density in ${}^{208}\text{Pb}$ inferred from electron scattering,³⁸ viz., $\rho_p(10\text{ fm}) \approx 10^{-4}$ protons/fm³. Thus our analysis of ($d, {}^6\text{Li}$) implies that about 1% of the protons at 10 fm in ${}^{208}\text{Pb}$ are associated with α clusters, at least on the time scale of nuclear reactions ($\approx 10^{-20}$ s). It is possible that the nuclear charge distribution exhibits nonuniformities in the nuclear periphery of this order of magnitude ($\approx 1\%$) due to α clustering. Such effects should be considered in problems involving nuclear quantum electrodynamics.

D. Super-heavy nuclei

A doubly closed-shell superheavy nucleus may be expected to have a reduced α width and effective α -cluster binding potential similar to that for ${}^{208}\text{Pb}$. There is a large uncertainty in Q_α ($A \approx 300$) of course, but taking Q_α ($Z = 114, N = 184$) = 7.0 MeV as indicated by some recent calculations,^{35,36} and utilizing our data for ${}^{208}\text{Pb} \rightarrow {}^{204}\text{Hg}_{\alpha.s.} + \alpha$, namely α -cluster bound state parameters and α widths, implies an α -decay half-life of $T_{1/2}^\alpha \approx 300$ years. This value depends strongly on the decay energy, and for $Q_\alpha = 7.0 \pm 0.5$ MeV we obtain $\log T_{1/2}^\alpha$ (years) = 2.5 ± 2 . This is to be compared with values $T_{1/2}^\alpha = 790$ years³⁶ and 400 to 4000 years³⁷ deduced from other means. Our data for excited states (Table II) suggest that a doubly magic superheavy nucleus might also have weak α -decay branches to excited states but we calculate these to be only $1 \pm 0.5\%$ for a 2^+ state at 400 keV.

We thank the scientific and operating staff of the Texas A&M Cyclotron Institute for their assistance. This work was supported in part by the National Science Foundation, Grant No. PHY78-07754.

- *Currently at Fermi National Accelerator Laboratory, Batavia, Illinois 60510.
- ¹H. J. Mang, *Annu. Rev. Nucl. Sci.* **14**, 1 (1964); *Clustering Phenomena in Nuclei II*, edited by D. A. Goldberg *et al.*, USERDA Report No. ORO-4856-25, 1975 (unpublished), p. 601; J. O. Rasmussen and I. Perlman, in α , β and γ -Spectroscopy, edited by K. Siegbahn (North-Holland, Amsterdam, 1964).
- ²D. F. Jackson and M. Rhoades-Brown, *Ann. Phys.* (N.Y.) **105**, 151 (1977); *Nature* **267**, 593 (1977).
- ³L. Milazzo-Colli *et al.*, *Nucl. Phys.* **A210**, 297 (1973); **A213**, 274 (1974); E. Gadioli *et al.*, *Phys. Rev. C* **16**, 1404 (1977).
- ⁴P. G. Roos *et al.*, *Phys. Rev. C* **15**, 69 (1977); D. Bache-lier *et al.*, *Nucl. Phys.* **A268**, 488 (1976); N. S. Chant, in *Proceedings of the Third International Conference on Clustering* (Winnipeg, Manitoba, 1978); p. 415.
- ⁵F. D. Becchetti *Proceedings of the Third International Conference on Clustering* (Winnipeg, Manitoba 1978), p. 308.
- ⁶F. D. Becchetti, L. T. Chua, J. Jänecke, and A. M. Vander Molen, *Phys. Rev. Lett.* **34**, 225 (1975).
- ⁷F. L. Milder, J. Jänecke, and F. D. Becchetti, *Clustering Phenomena in Nuclei II*, edited by D. A. Goldberg *et al.*, USERDA Report No. ORO-4856-25, 1975, p. 409; *Nucl. Phys.* **A278**, 72 (1977).
- ⁸W. Von Oertzen, in *Clustering Phenomena in Nuclei II*, edited by D. A. Goldberg, USERDA Report No. ORO-4856-25, 1975, p. 369.
- ⁹W. G. Davies *et al.*, *Nucl. Phys.* **A269**, 477 (1976); R. M. DeVries *et al.*, *Phys. Rev. Lett.* **35**, 835 (1975).
- ¹⁰M. Ichimura, A. Arima, E. C. Halbert, and T. Terasawa, *Nucl. Phys.* **A204**, 225 (1973).
- ¹¹K. T. Hecht and D. Braunschweig, *Nucl. Phys.* **A244**, 365 (1975).
- ¹²A. Arima and F. Iachello, *Ann. Phys.* (N.Y.) **99**, 253 (1976); *Phys. Rev. C* **16**, 2085 (1977).
- ¹³C. L. Bennett and H. W. Fulbright, *Phys. Rev. C* **17**, 2225 (1978).
- ¹⁴R. Betts, *Phys. Rev. C* **16**, 1617 (1977).
- ¹⁵J. Jänecke, F. Becchetti, D. Overway, and C. Thorn, in *Proceedings of the Tokyo Conference on Nuclear Structure* (1978), p. 358; *Proceedings of the Third International Conference on Clustering* (Winnipeg, Manitoba, 1978), p. 714.
- ¹⁶J. Jänecke, F. D. Becchetti, D. Overway, J. D. Coisart, and R. L. Spross (unpublished).
- ¹⁷C. Ellegaard, J. D. Garrett, and J. R. Lien, *Nucl. Phys.* **A307**, 125 (1978); J. Maher *et al.*, *Bull. Am. Phys. Soc.* **19**, 104 (1974), and private communication.
- ¹⁸E. R. Flynn, D. L. Hanson, R. V. Poore, S. D. Orbe-
sen, and D. A. Lind, *Phys. Lett.* **76B**, 197 (1978); E. R. Flynn, private communication.
- ¹⁹S. M. Smith, P. G. Roos, A. M. Bernstein, and Cyrus Moazed, *Nucl. Phys.* **A158**, 497 (1970).
- ²⁰Chin W. Ma and William W. True, *Phys. Rev. C* **8**, 2313 (1973).
- ²¹A. Pakkanen *et al.*, *Nucl. Phys.* **A184**, 157 (1972); D. Proetel *et al.*, *Nucl. Phys.* **A231**, 301 (1974); W. R. Hering *et al.*, *Phys. Rev. C* **14**, 1451 (1976); James E. Draper *et al.*, *ibid.* **16**, 1594 (1977); H. Toki *et al.*, *Nucl. Phys.* **A279**, 1 (1977).
- ²²Program DWUCK5, P. D. Kunz (unpublished); J. D. Comfort, private communication.
- ²³Program LOLA, R. M. DeVries, *Phys. Rev. C* **8**, 951 (1973).
- ²⁴K. I. Kubo and M. Hirata, *Nucl. Phys.* **A187**, 186 (1972).
- ²⁵J. W. Watson *et al.*, *Nucl. Phys.* **A172**, 513 (1971).
- ²⁶H. W. Fulbright *et al.*, *Nucl. Phys.* **A284**, 329 (1977); *Phys. Lett.* **53B**, 499 (1975); U. Strohmusch *et al.*, *Phys. Rev. C* **9**, 965 (1974); *Phys. Rev. Lett.* **34**, 968 (1975); R. M. DeVries *et al.*, *Phys. Lett.* **55B**, 33 (1975).
- ²⁷J. D. Childs, thesis, University of Pittsburgh, 1976 (unpublished); W. W. Daehnick, private communication.
- ²⁸L. T. Chua, F. D. Becchetti, J. Jänecke, and F. L. Milder, *Nucl. Phys.* **A273**, 243 (1976).
- ²⁹F. D. Becchetti, J. Jänecke, and C. Thorn, *Nucl. Phys.* **A305**, 313 (1978).
- ³⁰F. D. Becchetti and G. W. Greenlees, *Phys. Rev.* **182**, 1190 (1969).
- ³¹D. A. Goldberg, S. M. Smith, H. G. Pugh, P. G. Roos, and N. S. Wall, *Phys. Rev. C* **7**, 1938 (1973).
- ³²J. S. Lilley, *Phys. Rev. C* **3**, 2229 (1971); P. Mailandt, J. S. Lilley, and G. W. Greenlees, *ibid.* **8**, 2189 (1973).
- ³³Lynne McFadden and G. R. Satchler, *Nucl. Phys.* **84**, 177 (1966); F. M. Mann and R. W. Kavanagh, *Nucl. Phys.* **A255**, 287 (1975); G. M. Hudson and R. H. Davis, *Phys. Rev. C* **9**, 1521 (1974); B. D. Watson *et al.*, *Phys. Rev. C* **4**, 2240 (1971).
- ³⁴A. R. Barnett and J. S. Lilley, *Phys. Rev. C* **9**, 2010 (1974).
- ³⁵A. P. Lightman and W. J. Gerace, *Phys. Lett.* **30B**, 526 (1969).
- ³⁶E. O. Fiset and J. R. Nix, *Nucl. Phys.* **A193**, 647 (1972).
- ³⁷Daphne Jackson, E. J. Wolstenholme, L. S. Julien, and C. J. Batty (unpublished).
- ³⁸R. Hofstadter and H. R. Collard, *Nuclear Radii* (Springer, Berlin, 1967); C. J. Batty and G. W. Greenlees, *Nucl. Phys.* **A133**, 673 (1969).